Heliyon 7 (2021) e07468

Contents lists available at ScienceDirect

Heliyon

journal homepage: www.cell.com/heliyon

Research article

Bio-inspired gelatin/single-walled carbon nanotube nanocomposite for transient electrochemical energy storage: An approach towards eco-friendly and sustainable energy system

Rabeya Binta Alam, Md. Hasive Ahmad, Muhammad Rakibul Islam *

Department of Physics, Bangladesh University of Engineering and Technology (BUET), Dhaka, Bangladesh

ARTICLE INFO

Keywords:
Gelatin
Carbon nanotube
Biodegradable
Transient
Electrochemical properties

ABSTRACT

Wide-scale production of non-biodegradable e-waste from electrical appliances are causing great harm to the environment. The use of bio-polymer based nanomaterials may offer a promising approach for the fabrication of eco-friendly sustainable devices. In this work, gelatin/single walled carbon nanotube (Gel/SWCNT) nanocomposites were prepared by a simple and economic aqueous casting method. The effect of SWCNT on the structural, surface-morphological, electrical, and electrochemical properties of the nanocomposite was studied. Fourier transform infrared spectroscopy (FTIR) and field emission scanning electron microscope (FESEM) showed an improved degree of interaction between the SWCNTs and Gel matrix. The surface wettability of the nanocomposites was found to be changed from hydrophilic to hydrophobic in nature due to the incorporation of SWCNTs into the Gel matrix. The incorporation of SWCNTs was also found to reduce the DC resistivity of the nanocomposite by 4 orders of magnitude. SWCNTs also increase the specific capacitance of the nanocomposite from 124 mF/g to 467 mF/g at a current density of 0.3 mA/g. The electrochemical impedance spectroscopy analysis revealed an increase of the pseudo-capacitance increased from 9.4 μF to 31 μF due to the incorporation of SWCNT. The Gel/SWCNT nanocomposite showed cyclic stability with capacitive retention of about 98% of its initial capacitance after completing 2000 charging/discharging cycles at a current density of 100 mA/g. The nanocomposite completely dissolves in water within 12 h, demonstrates it as a promising candidate for transient energy storage applications. The Gel/SWCNT nanocomposite may offer a new route for the synthesis of eco-friendly, biodegradable, and transient devices.

1. Introduction

Though the electrical and electronics industry is presently emerging at a rocket speed, the aftermath is not quite pleasant. The junks or solid wastes produced from electrical appliances after their lifetime is named electronic waste or 'E-wastes' [1, 2]. With the recent booming in this industry, the amount of yearly production of E-wastes also got increased. Subsequently filling up the landfills, E-wastes are now endangering nature by taking place in the rivers, seas, and oceans [3, 4]. Most of the components of these wastes are produced from toxic and non-biodegradable materials, which are making them a constant threat to the nature [5]. The scraps derived from the E-wastes are mainly plastics, glass, and metals [3]. Synthetic plastics are considered as the greatest threat to nature in modern civilization for their non-biodegradable nature. Heavy metals like lead, mercury, cadmium, thallium, nickel, etc. are extremely harmful to any living being [6].

Some of the heavy metallic residues of e-wastes are tremendously hazardous (wastes produced from the battery of a device) and are harmful to living bodies and the natural environment not only in the present time but also for future generations [6]. As per an estimation by the UN, only in the year 2018, the overall discarded E-wastes from the whole world were approximately 50 million metric tons [3, 7]. So, to ensure a sustainable energy future it is a call of time to invent efficient novel materials for device applications (such as-sensor, actuator, battery, supercapacitor, etc.) that can meet the quality expectation with less or no harmful footprints on nature. To meet these demands, materials from nature-derived or renewable resources should be brought to the attention of the device manufacturing industries.

* Corresponding author.
E-mail address: rakibul@phy.buet.ac.bd (M.R. Islam).

https://doi.org/10.1016/j.heliyon.2021.e07468
Received 17 May 2021; Received in revised form 12 June 2021; Accepted 30 June 2021

A number of devices such as sensors, actuators, drug delivery devices, etc. used in the biomedical and environmental sector need to perform efficiently for a certain period of time and then disappear from the system without causing any hamper [8, 9, 10]. They do not need a constant source of energy as well as a long-lasting structural body. These devices should have made with fully bio-derived materials that can perform swiftly for the desired period of time and then disappear from the system without leaving any harmful footprints. These kinds of devices are called transient devices [11, 12]. It is an emerging and promising field where the invention of bio-derived novel materials appropriates for use in the devices is the main focus. More recently, electronic devices fabricated from transient materials, named transient electronics have gained significant research attention [11, 13].

Polymer obtained from bio-derived sources is the most suitable candidates for transient device applications [8, 12, 13, 14]. More specifically, bio-inspired polymer nanocomposites is a special class of materials that consist of nature-derived polymer and are of particular interest because of their environment-friendly features. Polymers present in different biological bodies are abundant, cost-efficient, and nature-friendly materials possessing all the advantages of polymers like flexibility, heat and electron resistivity, mechanical strength along with lightweight, etc. [15, 16, 17]. So far, a number of biopolymers, such as cellulose, starch, chitosan, gelatin, etc. [8, 12, 13, 14] have shown transient device applications. Among them, gelatin is one of the most promising biopolymers synthesized from partial hydrolysis of collagen present in bones of animal body found its applications in a number of fields including food packaging, drug delivery, bio implant, etc. [18, 19, 20]. In this article, we will focus on the transient energy storage performance of gelatin bio-polymer.

The different physical properties of the polymer can be tuned, improved and its area of applicability can further be widened by adding fillers into the polymer matrix. Recently, nanostructured materials have gained significant research attention as filler materials because of possessing unique and promising physical, chemical, structural, and mechanical characteristics [21, 22, 23]. Among the available alternatives, single wall carbon nanotube (SWCNT), rolled up cylinder of a single layer of graphene, has considered as a popular building block for the synthesis of bioinspired polymer-based nanocomposites because of their unique electronic properties, high thermal conductivity together with extraordinary mechanical strength and flexibility [24, 25, 26].

The high electronic conductivity together with a large surface area allow accumulation of charge carrier at the electrode surface and the ion at the electrolyte that forms electric double-layer capacitance [27, 28, 29]. Because of these outstanding properties SWCNT is considered as an ideal candidate for electrical energy storage purposes [30, 31].

The properties and performance of a nanocomposite depend on its synthesis process. Some processing techniques such as surface activation, modification, in situ polymerization, etc. are laborious, expensive, involve complex processing steps, and are often not easy for industrial applicatons [32, 33]. Therefore, to get the best result for being benefitted, a route of easy processing should also be determined. The solution cast technique offers an easy, high yield, and cost-effective route for the production of novel polymer nanocomposites [34].

Although transient electronics is an emerging and promising field of research, only a few attempts have been reported till date [34, 35, 36, 37]. However, to the best of our knowledge, no work has been reported yet on the study of electronic energy storage behavior of the bio-inspired gelatin/SWCNT nanocomposites. In this work, we synthesized bio-inspired gelatin/SWCNT nanocomposite following a facile route of production-'aqueous solution processing'. The effect of the concentration of SWNTs on the chemical bonding, surface morphology, electrical transport, and electrochemical performance of the nanocomposites were evaluated. Cyclic voltammetry (CV), galvanostatic charging-discharging (GCD), and electrochemical impedance spectroscopy (EIS) analysis were conducted in a three-electrode system in 0.1 M KCl electrolyte solution to study the electrochemical properties of the nanocomposites. The incorporation of SWCNTs was found to significantly enhance the pseudocapacitance of the nanocomposites and thereby increase the specific capacitance. Besides, the cyclic stability, rate capability as well as bio-degradability has also been discussed in detail.

2. Experimental section

2.1. Material

Gelatin powder (type B from bovine skin, ~200 Bloom) and glycerol (98% pure) were obtained from Sigma-Aldrich. Well-dispersed aqueous suspension of single wall carbon nanotube (concentration ~50 μg/mL) was obtained from Brewer Science. The solution contains mostly individual SWNTs with an average length of ~1–2 μm and the diameter of the SWCNTs varies between 0.5– 5.0 nm [26, 28].

2.2. Nanocomposite preparation

A solution of gelatin and glycerol was made where the ratio of gelatin to glycerol was kept at 3:1. Gelatin was perfectly dissolved by applying a little heat along with mechanical stirring. Then the well-dispersed aqueous solution of SWCNT was incorporated in this solution at different proportions (50μL, 100μL, and 200μL) to make the nanocomposite. Heat was applied to evaporate the excess water from the solution and stirring was confirmed throughout the process to ensure the proper dispersion of SWCNTs while film-forming. The obtained solution was then cast on a glass Petri dish and dried with open airflow in a safe place at room temperature for at least 72 h. Afterward, these samples were vacuum conditioned at 740 mm Hg for about 1 day. Then the films were peeled out carefully from the glass slide and were ready for characterization. Figure 1 represents a schematic illustration of the nanocomposite preparation and formation methodology in the above-mentioned process. Here the samples containing 0 μL, 50 μL, 100 μL, and 200 μL SWCNT is termed as A, B, C, and D respectively.

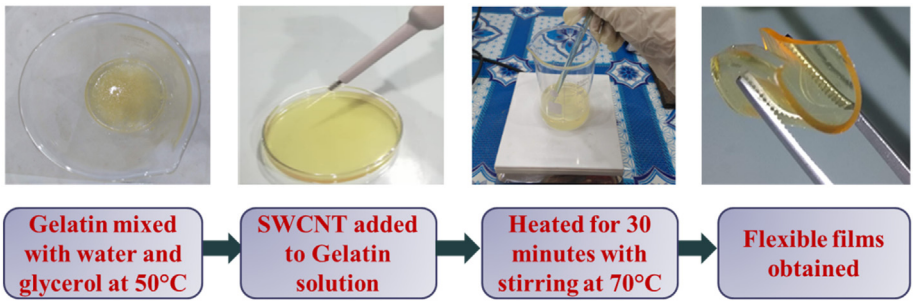

Figure 1. Schematic illustration of the different steps in the synthesis of Gel/SWCNT nanocomposites.

2.3. Electrode preparation

A glassy carbon electrode was used as the current collector in this preparation. The electrode was cleaned by rubbing on a smooth paper in an 8-fashioned way and the mass of the electrode was measured in a digital weight machine which has an accuracy of up to 0.0001 g. Then a tiny drop of the prepared material was deposited directly on the top contact surface of the electrode. Then the electrode was dried at room temperature for 2 h. Finally, vacuum dried for 1 h, and then again, the mass of the electrode was measured. Mass of the deposited material was found from the difference of masses measured from before and after the deposition.

2.4. Characterization

The presence of different groups in the cross-linked nanocomposites was studied by Fourier transform infrared spectroscopy (FTIR) analysis. The FTIR analysis was performed in attenuated total reflection (ATR) mode by using a (Shimadzu IRSpirit) spectrophotometer at a spectrum range of 640–4000 cm^{-1}.

The surface morphology of the cross-section of Gel/SWCNT nanocomposite was studied by a field emission scanning electron microscope (FESEM) (JEOL JSM-7600F) at an accelerating voltage of 5 kV. Before imaging, the composites were sputtered by a thin layer of gold/palladium.

A homemade Van der Pauw four-probe setup was used to evaluate the DC electrical properties of the nanocomposite. The resistivity, ρ of the composite were estimated by the equation, $\rho = 2\pi s(V/I)$ [38]. Where V is the applied potential between the innermost probes, I is the measured current obtained between the external pair of probes, and s is the probe-spacing.

2.5. Electrochemical measurement

All the electrochemical properties were analyzed in a three-electrode system: a glassy carbon electrode was used as the working electrode, a platinum foil plate (1 × 1 cm^2) serve as the counter electrode, and a silver/silver chloride electrode (Ag/AgCl) was used as the reference electrode, and 0.1 M KCl was used as an ionic aqueous electrolyte solution. The cyclic voltammetry (CV), galvanostatic charge/discharge (GCD), and electrochemical impedance spectroscopy (EIS) were measured by using CS310 Electrochemical Working Station (corrtest, china). The CV and GCD were observed over a voltage range from -0.2 V to 0.7 V, and the EIS data was taken in the frequency range between 0.01– 100,000 Hz by applying an AC voltage perturbation of 10 mV. 2000 GCD cycles were performed at a current density of 100 mA/g from -0.2 V to 0.7 V voltage window. All the electrochemical tests were carried out at room temperature.

The specific capacitance C_S of the biocomposites was estimated by integrating the area under the cyclic voltammogram (CV) curves according to the following equation,

$$Cs = \frac{1}{v.m.(V2-V1)} \int_{V1}^{V2} i(V)dV \text{ [39, 40];}$$

where v is the voltage scan rate, m is the mass of the active material and $(V_2 - V_1)$ is the applied potential window.

The specific capacitance can also be calculated from the galvanostatic charging-discharging curve, using the equation,

$$Cs = \frac{Idisch}{m} \frac{dt}{dV} \text{ [39, 41];}$$

where I_{disch} is the discharge current and dV/dt is the gradient of the GCD curve during discharging.

The Energy density, E and Power density, P are calculated with the following formula,

$$E = \frac{Cs \times \Delta V^2}{7.2} \text{ [39, 42];}$$

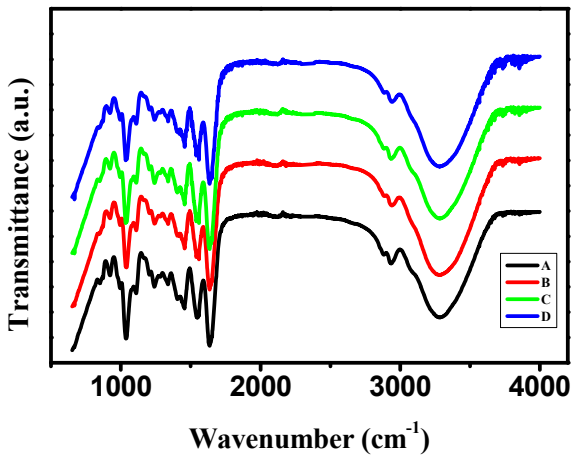

Figure 2. FTIR Spectra of Gel/SWCNT nanocomposites for different amounts of SWCNT filler content.

$$P = \frac{E \times 3600}{\Delta t} \text{ [39, 42];}$$

Where, C_S = Specific capacitance calculated from GCD graph; ΔV = Operating voltage window and Δt = Discharge time.

3. Result and discussion

3.1. Fourier transform infrared spectroscopy

FTIR spectroscopy was carried on the sample's surface to analyze the structural properties of the prepared Gel and Gel/SWCNT samples. Figure 2 illustrates the FTIR spectra of all the nanocomposite samples from 650 cm^{-1} to 4000 cm^{-1} wavenumber range. From Figure 2, a broad and deep absorption peak is observed from 3100 cm^{-1} to 3600 cm^{-1} which is the corresponding peak for the strong stretching vibration of –OH group of the trapped water from solution remained in the sample [20, 43]. Other characteristic peaks for the peptide groups of gelatins such as amide-A, B, I, II, III are also noticed here. The peak at 2935 cm^{-1} for amide-A represents the NH- stretching coupled with hydrogen bonding. The peak of Amide B situated at 2883 cm^{-1} originates from the stretching of CH- and NH_3^+ [43]. Absorption peaks located at 1638 cm^{-1}, 1542 cm^{-1}, and 1254 cm^{-1} correspond to the amide-I, II, III band respectively. Amide- I arise from the C=O stretching vibrations whereas amide –II represents bending of N–H groups associated with stretching of C–N groups. Amide –III arises due to vibration of CH_2 group [44]. The addition of SWCNT doesn't add any additional peak may be due to low concentration. But the increase of intensity and a slight shift of the peak's position in accordance to SWCNT concentration indicates a possible interaction has occurred among the SWCNTs and the –OH group of water and glycerol of the solution along with NH_2– groups of gelatins. Thus, SWCNTs allocate themselves well in these intermediate locations.

3.2. Surface morphology analysis

The morphology of the cross-sectional surfaces Gel/SWCNT nanocomposites was studied by the FESEM and is presented in Figure 3. The surface of the pure Gel was found to be smooth. SWCNT was observed for sample B, maybe due to the use of a vary low concentration of SWCNT. However, traces of SWCNTs were observed for samples C and D. With the increase of SWCNT filler concentration the roughness of the film got increased. This type of morphological feature has also been observed in Gel/CNT nanocomposites, reported earlier and occurred due to the formation of interfacial bonding between carbon nanotube and the polymer matrix [45, 46]. Furthermore, the increase of the nanofiller concentration was found to increase the roughness of the composite surface.

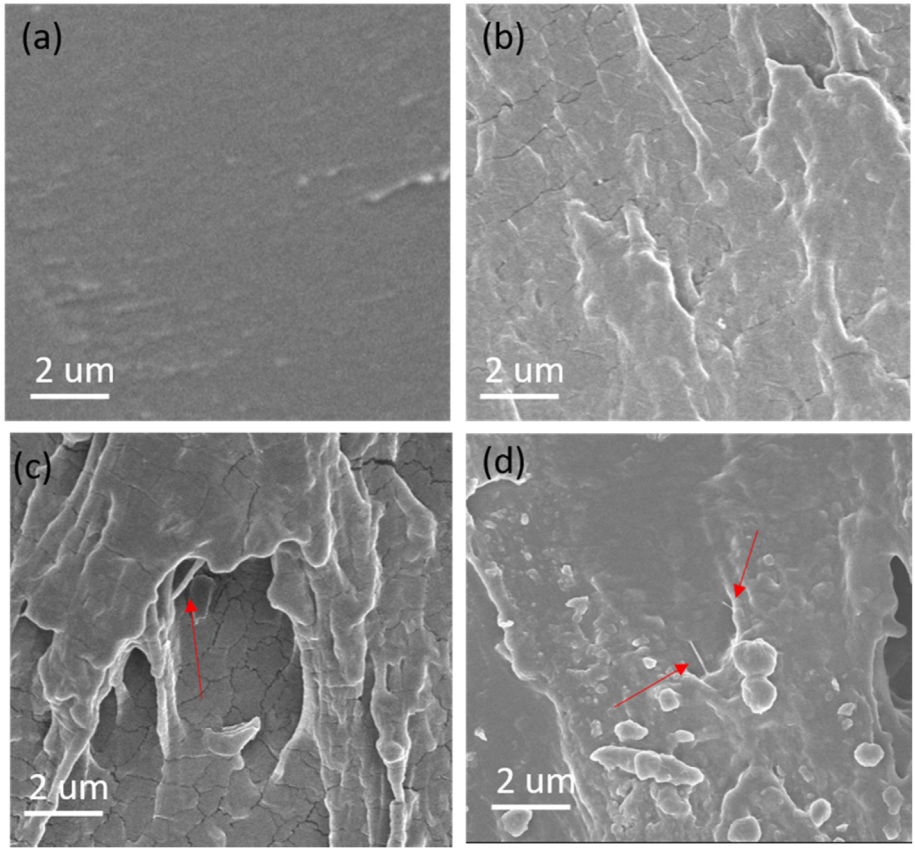

Figure 3. FESEM images of Gel/SWCNT films with different filler concentrations: (a) sample A, (b) sample B, (c) sample C, and (d) sample D. Presence of SWCNTs are indicated by arrows.

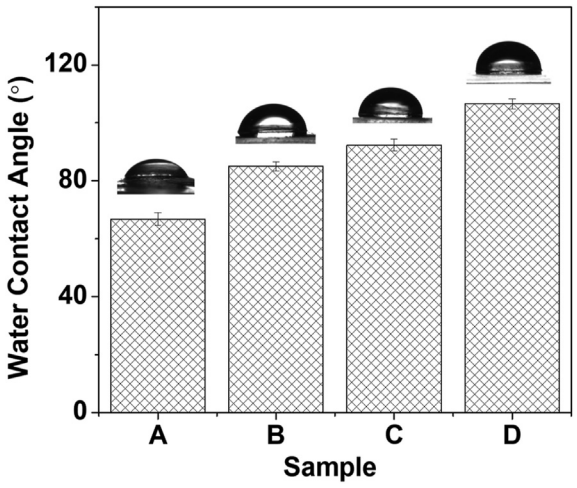

Figure 4. The change in the water contact angle of Gel/SWCNT nanocomposites for different concentrations of SWCNTs.

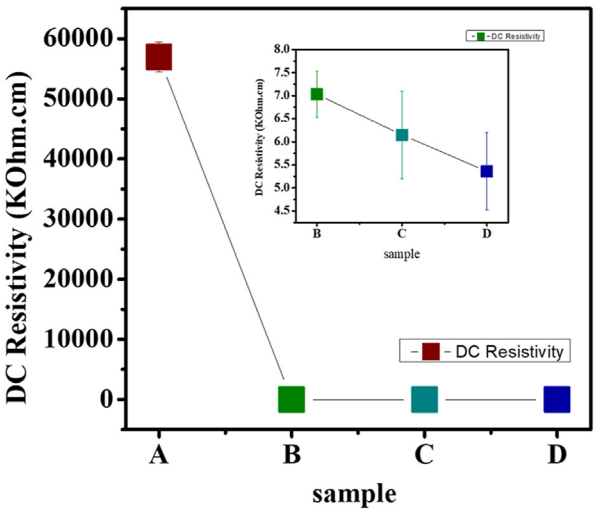

Figure 5. Variation of the DC Resistivity among Gel and Gel/SWCNT nanocomposites as a function of SWCNT content.

3.3. Surface wettability

The surface wettability property of the nanocomposites was studied by measuring their corresponding contact angle and the result is displayed in Figure 4. The water contact angle (WCA) for the materials showed a transition from hydrophilic to a moderately hydrophobic character due to the incorporation of SWCNT into the Gel sample. This might be because of the uneven surface and surface roughness of the sample with SWCNT [29, 47]. The contact angle for Gelatin was found to be 66.81° which confirmed its hydrophilic nature, but with the incorporation of SWCNTs, WCA rose. After incorporating 200μL of SWCNT, the WCA rose to 106.48° and the nanocomposite became hydrophobic in nature. This happens as the SWCNTs are generally highly hydrophobic in nature due to their non-polar structure [10, 48], so only a trifling amount of filler can make the Gel material moderately hydrophobic. The carboxyl groups of SWCNTs along with the hydroxyl groups of gelatins is responsible for the lesser water uptake [10, 49, 50].

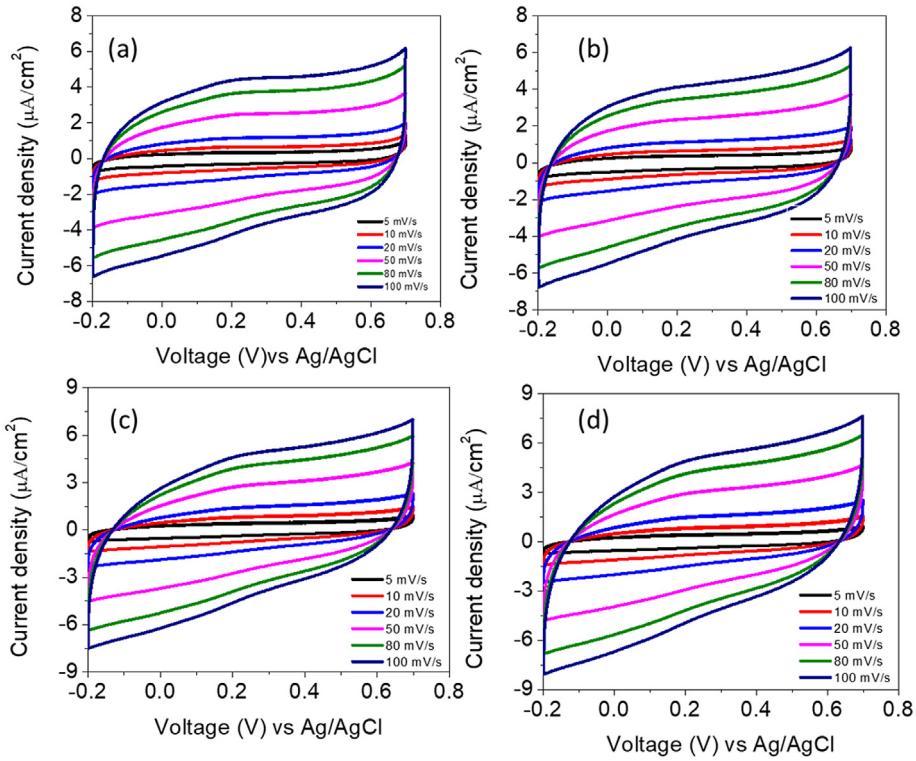

Figure 6. Cyclic Voltammetry of a) Gel, b) Gel/50μL SWCNT, c) Gel/100μL SWCNT, and d) Gel/200μL SWCNT at different voltage scan rates.

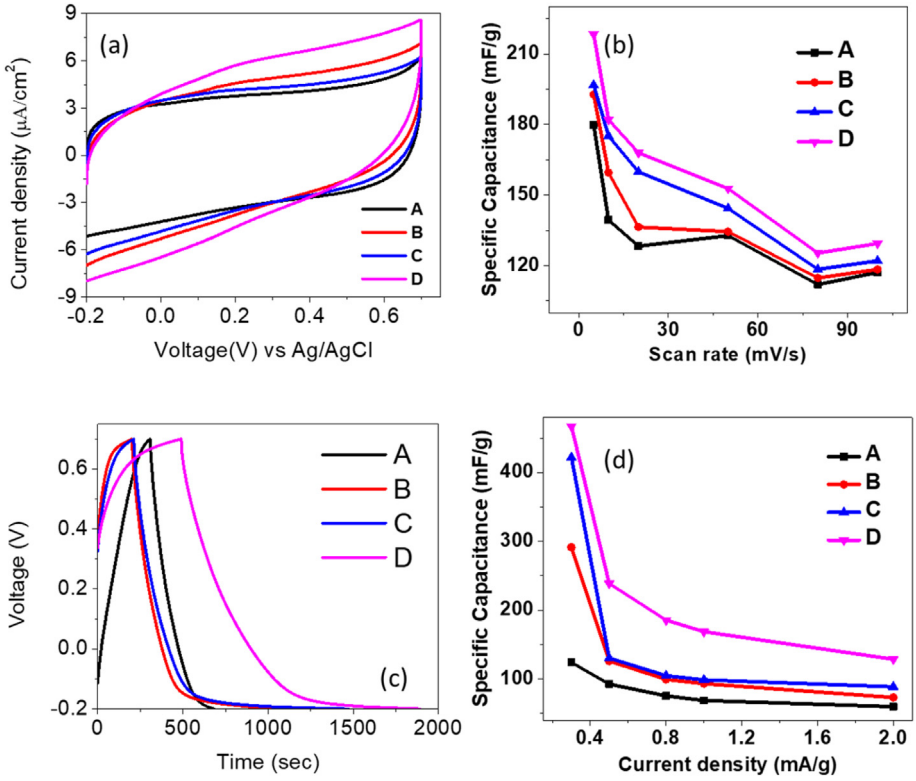

Figure 7. Variation of (a) Cyclic voltammetry curve at a sweep rate of 100 mV/s , (b) specific capacitance estimated from the CV curve at different voltage scan rates, (c) galvanometric charging-discharging curve at a current density of 0.3 mA/g, (d) specific capacitance estimated from GCD curve for all the samples.

3.4. DC resistivity

The variation of the DC resistivity of the Gel and Gel/SWCNT composites is shown in Figure 5. The DC resistivity of the nanocomposites significantly decreased for the incorporation of SWCNTs in the Gel matrix. Sample B with only 50 μL of SWCNT content, exhibited an insulator to conductor transition in the nanocomposites. The nanocomposites displayed a dramatic decrease of around 4 orders of magnitude in their DC resistivity. For the pure gelatin sample, A, DC resistivity was measured around 57 MΩ cm. This value decreased down to 7 kΩ-cm for the incorporation of only 50 μL SWCNT in the polymer matrix. Sample D with 200 μL of SWCNT content showed DC resistivity of around 5.4 kΩ-cm. Gelatin is a biopolymer and electrically behaves like an insulator [49]. But the incorporation of SWCNT fillers gradually builds a pathway for electrons to pass through the insulating polymer complex. The main reason for this outcome is the atomic structure of SWCNTs. SWCNTs are the folded form of sp^2 hybridized graphene sheets and in their atomic arrangement, there remains one free electron that shows electronic properties [51]. When a voltage is applied to the nanocomposites the unhybridized electron takes part in conducting electricity from one tube to another throughout the polymer matrix through different processes like tunneling, hopping, or jumping [52].

3.5. Electrochemical properties

3.5.1. Cyclic voltammetry

Cyclic voltammetry was conducted to investigate the electrochemical properties of the prepared materials. Figure 6(a-d) shows the CV curves of the four samples- A, B, C, and D respectively at different scan rates: 5, 10, 20, 50, 80 and 100 mV/s in the voltage range from -0.2 V to 0.7 V. Observed CV curves found to be near rectangular and approximately symmetric in shape. Figure 7(a) gives a comparative illustration of all the nanocomposite materials at a voltage sweep rate of 100 mV/s. The corresponding values of the specific capacitance (C_s) at different scan rates for all the samples were measured and listed in Figure 7(b). From the figure, it was found that the material holds a larger value of C_s in a lower scan rate. At 5 mV/s the value of C_s was estimated to be 180, 193, 197, and 219 mFg^{-1} for Gel, Gel/50μL SWCNT, Gel/100μL SWCNT, and Gel/200μL SWCNT nanocomposites respectively. This is due to the ions of the electrolyte have enough time for getting diffused into the SWCNT intermolecular regions at low scan rates [37, 53]. Thus, ions can utilize more surface area of SWCNTs rather than they can in higher scan rates [54]. At higher scan rates the charging and discharging happens too rapidly to diffuse the ions properly and the value of C_s decreases. At 100 mV/s, for sample D the value of C_s was found to be 129.42 mF/g where the rate capability is about 40% of the initial value at 5 mV/s. Although the shape of the CV curve is nearly rectangular, a slight bump of redox peak is observed at around 2.5V. This peak and the cumulative quasi-rectangular shape of the CV curves with the incorporation of a higher amount of SWCNT in the Gel matrix confirms the existence of pseudo-capacitance [29, 55]. Pseudo-capacitance could be raised from the interaction of SWCNT with the open bonds of the gelatin skeleton in the ionic electrolyte [55]. The collective effect of forming a capacitive layer and pseudo-capacitance is the reason of the increase of the C_s with the incorporation of SWCNT [56].

3.5.2. Galvanometric charging discharging

To have more substantial information about the electrochemical properties of the Gel/SWCNT materials, galvanometric charging and discharging (GCD) was performed. The GCD operated at -0.2V–0.7V voltage window at different current densities (0.3, 0.5, 0.8, 1, and 2 mA/g), Figure 7(c) gives a comparative illustration of GCD of all the nanocomposite materials at 0.3 mA/g current density and all the corresponding specific capacitance, Cs values shown in Figure 7(d) exhibits an increase of Cs with SWCNT increment in the Gel matrix. Here also observed the specific capacitance is higher at lower current densities. Cs of about 124, 291, 422, and 467 mF/g were found for samples A, B, C, and D respectively at 0.3 mA/g current density. The reason is that at lower current density lesser amount of ions come close to a certain portion of the surface area of the SWCNT wall and can diffuse themselves properly [42, 57]. Whereas at higher surface area more ions traffic at certain portion of SWCNT wall and cannot diffuse themselves enough into the SWCNT surface [35, 57, 58]. As a result, the value of Cs lowers down. Also, the charging-discharging rate accelerates at the higher current densities results in a lower value of Cs. At a higher current density of 2 mA/g, the value of Cs was calculated 60, 73, 88, and 128 mF/g for the sample A, B, C, and D respectively. The specific capacitance of the highest SWCNT contained sample increases by 4 times than that of the pure Gel sample as the SWCNTs form a conductive channel throughout the electrode material and increase the ion transportation [58]. The distorted triangular shape of the GCD curve also confirms the pseudo-capacitance of the nanocomposites as discussed in the previous subsection [29, 55, 56].

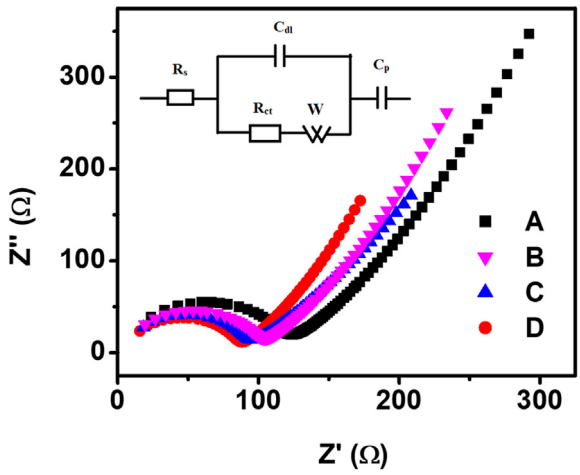

Figure 8. The best fitted curves of the complex impedance spectra (Nyquist plot of all the samples were taken from 0.01 Hz to 10^6 Hz). The inset shows the equivalent circuit used for simulation.

3.5.3. Electrochemical impedance spectroscopy

Nyquist plots were used to analyze the electrochemical impedance of the nanocomposite samples. To evaluate the contribution of different electrical component parts in the Nyquist plot a simulation was run and the best-fitted curves along with the equivalent circuit are shown in Figure 8. Corresponding values of the elements of the equivalent circuit are recorded in Table 1. Different portions of the Nyquist plot carry different information about the sample's electrochemical status according to the applied frequency. In the high-frequency region, the point where the Nyquist plot intercepts the real axis represents the value of combined series resistance, R_s; this value is the combination of the actual resistance of the electrode material, the resistance of the electrolyte and contact resistance of the electrode, and current collector [55, 59]. The value of R_s tends to decrease with the incorporation of SWCNTs in the polymer matrix from 7.45 Ω for Gel to 7.41 Ω for Gel/200μL SWCNT nanocomposite. SWCNTs might have created an easy route for current collectors to decrease the R_s value [50]. The semi-circle in the high-frequency region is indicative of the electrode conductivity and the charge transfer resistance of the electrode material [50, 57]. The radius of the semi-circle embodies the value of charge transfer resistance, R_{ct} [59]. The value of R_{ct} obtained from the simulation are 106.60 Ω, 88.98 Ω, 81.33 Ω, and 74.80 Ω for samples A, B, C, and D respectively. The extraordinary electric conductivity of SWCNTs helps to decrease the charge transfer resistance of the electrode [59]. The semicircular shape arises for a parallel relation of C_{dl} with $R_{ct.}$ C_{dl} is the capacitance of the double layer formed near the electrode-electrolyte interaction area [33, 59]. The fitted values obtained for C_{dl} are increased from 3.76 nF for Gel

Table 1. The values of the different components of the equivalent circuit for different Gel/SWCNT sample sobtained from simulation.

Sample	R_s (Ohm)	C_{dl} (nF)	R_{ct} (Ohm)	C_P (μF)
A	7.45	3.76	106.60	9.40
B	7.44	4.85	88.98	12.77
C	7.43	5.35	81.33	21.07
D	7.41	6.46	74.80	30.90

to 6.46 nF for the Gel/200μL SWCNT nanocomposite. The internal spaces where SWCNTs located might have created a charge capacitive region and thus C_{dl} value increased [33, 59]. In the intermediate frequency region, the nearly 45° slope of the curves is described as the Warburg resistance region, which represents the ion diffusion/transport on the electrolyte and electrode contact surface [60, 61]. In the low-frequency region, the capacitive behavior dominates as the bulk capacitance of the nanocomposite material, which is mainly pseudo-capacitance, C_p took place [55, 56]. The C_p value of the Gel/200μL SWCNT electrode (30.9 μF) increased more than three times the value obtained for Gel electrode (9.4 μF). Overall, as electrode material, the prepared nanocomposites display well capacitive behavior.

3.5.4. Cyclic stability and Ragone plot

Figure 9(a) displays capacitance retention of the Gel/200μL SWNT nanocomposite and the sample retains 98% of its maximum capacitance

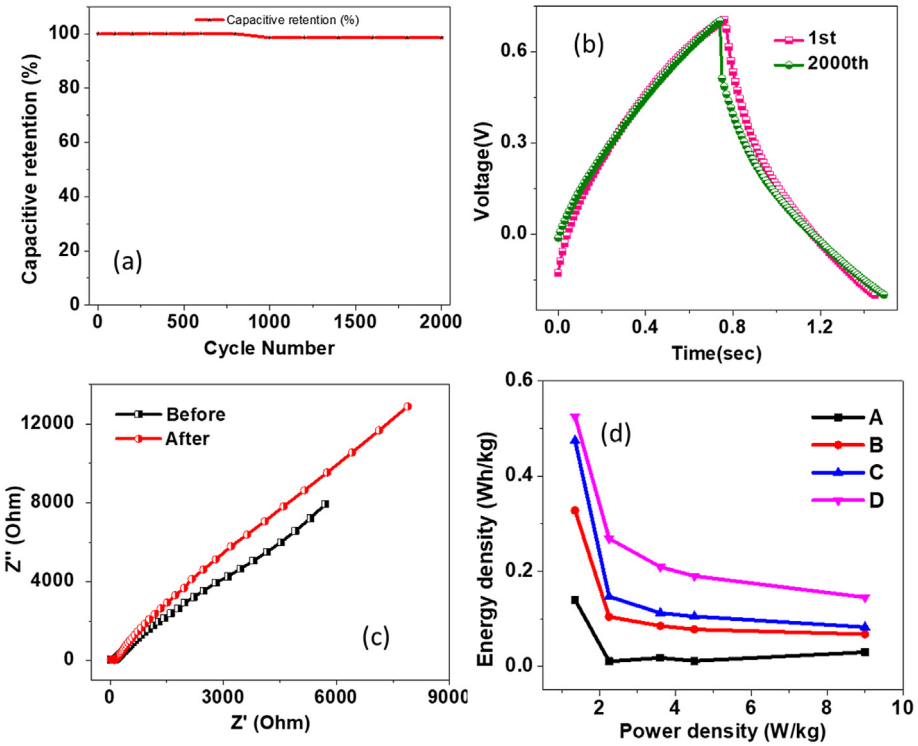

Figure 9. (a) The capacitive retention for 2000 cycle of GCD; (b) the GCD curves for the 1st and the 2000th cycle, (c) the Nyquist plots before and after 2000 cycle of the GCD performed, (d) Ragone plot of the nanocomposites.

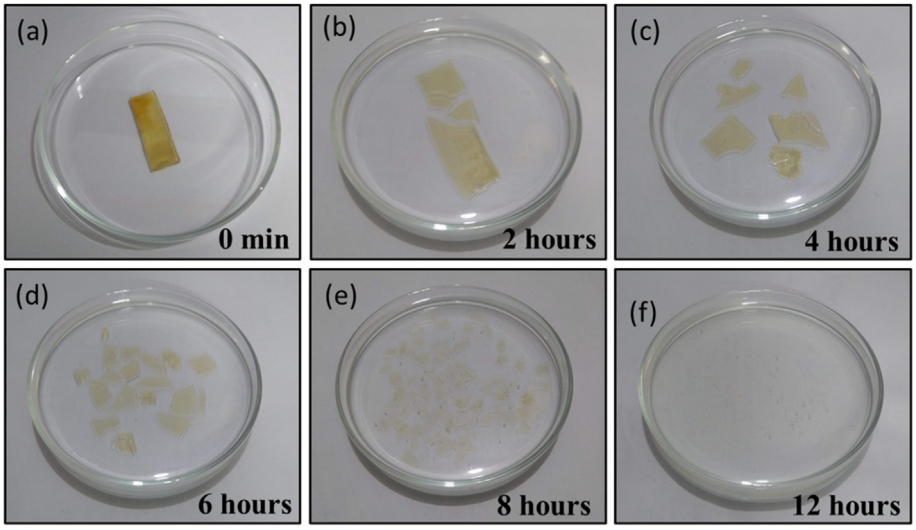

Figure 10. (a)–(f). Biodegradability test of the Gel/SWCNT samples in DI water.

after completing 2000 charging/discharging cycles at 100 mA/g current density. Figure 9(b) reveals the almost unchanged shape of the 1st and 2000th charging/discharging cycle. Then again, Figure 9(c) shows the EIS performed before and after 2000 GCD cycles. The series resistance of them remains nearly similar. The minor alteration of the resistance happens as some faradaic reaction or corrosion occurs on the electrolyte-electrode material surface [35, 57]. The slope of the Warburg resistance gets more inclined as the diffusion of ions from the faradaic reaction increases on the contact surface [61]. This impressive cyclic stability with long cycle life enhances their compatibility as an electrode material of supercapacitor.

From the Ragone plot 9(d) it is observed that the energy density of the Gel/SWCNT nanocomposites decreases with the increase of power density from 1.35 to 9 W/kg with the current densities increase from 0.3 to 2 mA/g. The nanocomposite with 200μL SWCNT exhibited an energy density decrease from 0.53 to 0.16 Wh/kg in the power density range. Maybe a greater concentration of SWCNTs could have been made a significant difference in the energy density.

3.6. Biodegradability analysis

Figure 10 (a) to (f) shows the degradation of Gel/SWCNT nanocomposite film with respect to time in DI water at room temperature. It took about 12 h to fully and safely disappear a 30 × 10 × 1 mm^3 film from the system. Biopolymers like gelatin are substituted or incorporated with some hydrophilic groups such as amino acid group, alcoholic group, etc. into their backbone that can dissolve, disperse, or swell in water [41, 62]. The swelling of the gelatin sample is understandable by comparing Figures 10(a) and 10(b). At that point, the swelled film breaks into pieces only by a gentle stirring 10(c). A gentle stirring for few seconds was performed every 2 h and the pictures were taken. Finally, the film was fully dissolves into water without remaining any trace after 12 h.

From the above discussion, it is clear that the incorporation of SWCNT into the Gel matrix can improve the electrochemical performance of the nanocomposite. The observed specific capacitance of the nanocomposite is quite low and this because of the low concentration of SWCNT nanofiller used in the polymer matrix. The capacitive performance of the nanocomposite can be further be improved by increasing the SWCNT nanofiller concentrations in the polymer.

4. Conclusion

A biodegradable, novel (Gel/SWCNT) nanocomposites were synthesized by a facile synthesis process. The structural and surface properties analysis demonstrate improved interaction between the polymer and the SWCNT filler. Significant reduction in the DC Resistivity due to incorporation of SWCNT causes electron and ion adsorption into the insulator biopolymer matrix resulting in improved electrochemical performance. The Gel/SWCNT nanocomposite offers excellent cyclic stability with a retention of 98% of its initial capacitance value even after 2000 cycles of operation. The Gel/SWCNT nanocomposite may offer a promising route for the synthesis of environment-friendly, biodegradable and transient energy storage devices.

Declarations

Author contribution statement

Rabeya Binta Alam: Conceived and designed the experiments; Performed the experiments; Analyzed and interpreted the data; Wrote the paper.

Md. Hasive Ahmad: Performed the experiments; Analyzed and interpreted the data.

Muhammad Rakibul Islam: Conceived and designed the experiments; Analyzed and interpreted the data; Contributed reagents, materials, analysis tools or data; Wrote the paper.

Funding statement

This research did not receive any specific grant from funding agencies in the public, commercial, or not-for-profit sectors.

Data availability statement

Data will be made available on request.

Declaration of interests statement

The authors declare no conflict of interest.

Additional information

No additional information is available for this paper.

References

[1] R.A. Patil, S. Ramakrishna, A comprehensive analysis of e-waste legislation worldwide, Environ. Sci. Pollut. Res. 27 (13) (2020) 14412–14431.
[2] A. Chatterjee, J. Abraham, Efficient management of e-wastes, Int. J. Environ. Sci. Technol. 14 (1) (2017) 211–222.
[3] S. Luhar, I. Luhar, Potential application of E-wastes in construction industry: a review, Construct. Build. Mater. 203 (2019) 222–240.
[4] P. Kiddee, R. Naidu, M.H. Wong, Electronic waste management approaches: an overview, Waste Manag. 33 (5) (2013) 1237–1250.
[5] F. Gu, B. Ma, J. Guo, P.A. Summers, P. Hall, Internet of things and Big Data as potential solutions to the problems in waste electrical and electronic equipment management: an exploratory study, Waste Manag. 68 (2017) 434–448.
[6] Q. Liu, et al., Chromosomal aberrations and DNA damage in human populations exposed to the processing of electronics waste, Environ. Sci. Pollut. Control Ser. 16 (3) (2009) 329–338.
[7] B. Bakhiyi, S. Gravel, D. Ceballos, M.A. Flynn, J. Zayed, "Has the question of e-waste opened a Pandora's box? An overview of unpredictable issues and challenges, Environ. Int. 110 (October) (2018) 173–192.
[8] G. Zhao, Z. Wang, H. Wang, H. Zhao, Y. Fu, J. Yang, Effect of doping nanoparticles on the output force performance of chitosan-based nanocomposite gel actuator, Polym. -Plast. Technol. Mater. 58 (9) (2019) 967–977.
[9] H. Bagheri, A. Afkhami, H. Khoshsafar, A. Hajian, A. Shahriyari, Protein capped Cu nanoclusters-SWCNT nanocomposite as a novel candidate of high performance platform for organophosphates enzymeless biosensor, Biosens. Bioelectron. 89 (2017) 829–836.
[10] Y. Yan, et al., Effect of multi-walled carbon nanotubes on the cross-linking density of the poly(glycerol sebacate) elastomeric nanocomposites, J. Colloid Interface Sci. 521 (2018) 24–32.
[11] K.K. Fu, Z. Wang, J. Dai, M. Carter, L. Hu, Transient electronics: materials and devices, Chem. Mater. 28 (11) (2016) 3527–3539.
[12] S.W. Hwang, et al., High-performance biodegradable/transient electronics on biodegradable polymers, Adv. Mater. 26 (23) (2014) 3905–3911.
[13] G. Lee, et al., Fully biodegradable microsupercapacitor for power storage in transient electronics, Adva. Energy Mater. 7 (18) (2017) 1–12.
[14] F. Quero, et al., Stress transfer and matrix-cohesive fracture mechanism in microfibrillated cellulose-gelatin nanocomposite films, Carbohydr. Polym. 195 (2018) 89–98.
[15] J. Brady, T. Drig, P.I. Lee, J.X. Li, Polymer Properties and Characterization, 2017.
[16] S. Chandran, et al., Processing pathways decide polymer properties at the molecular level, Macromolecules 52 (19) (2019) 7146–7156.
[17] D.T. Gentekos, R.J. Sifri, B.P. Fors, Controlling polymer properties through the shape of the molecular-weight distribution, Nat. Rev. Mater. 4 (12) (2019) 761–774.
[18] M.M. Rahman, Preparation of carbon nanotube reinforced gelatin-chitosan-hydroxyapatite biocomposite for bone tissue engineering, Open Access J. Biomed. Eng. Biosci. 1 (3) (2018) 66–72.
[19] K. Ren, Y. Wang, T. Sun, W. Yue, H. Zhang, Electrospun PCL/gelatin composite nanofiber structures for effective guided bone regeneration membranes, Mater. Sci. Eng. C 78 (2017) 324–332.
[20] C. Rajkumar, B. Thirumalraj, S.M. Chen, H.A. Chen, A simple preparation of graphite/gelatin composite for electrochemical detection of dopamine, J. Colloid Interface Sci. 487 (2017) 149–155.
[21] X. Xu, J. Zhou, J. Jestin, V. Colombo, G. Lubineau, Preparation of water-soluble graphene nanoplatelets and highly conductive films, Carbon N. Y. 124 (2017) 133–141.
[22] A. Journal, Bionanocomposite: A Review Bionanocomposite: A Review 5 (December) (2017) 1–3.
[23] K. Müller, et al., Review on the processing and properties of polymer nanocomposites and nanocoatings and their applications in the packaging, automotive and solar energy fields, Nanomaterials 7 (2017) 4.

[24] P. Stokes, M.R. Islam, S.I. Khondaker, Low temperature electron transport spectroscopy of mechanically templated carbon nanotube single electron transistors, J. Appl. Phys. 114 (8) (2013) 1–7.
[25] B.K. Sarker, M.R. Islam, F. Alzubi, S.I. Khondaker, Fabrication of aligned carbon nanotube array electrodes for organic electronic devices, Mater. Express 1 (1) (2011) 80–85.
[26] M.R. Islam, D. Joung, S.I. Khondaker, Towards parallel fabrication of single electron transistors using carbon nanotubes, Nanoscale 7 (21) (2015) 9786–9792.
[27] M.R. Islam, K.J. Kormondy, E. Silbar, S.I. Khondaker, A general approach for high yield fabrication of CMOS-compatible all-semiconducting carbon nanotube field effect transistors, Nanotechnology 23 (12) (2012).
[28] M.R. Islam, S.I. Khondaker, Recent progress in parallel fabrication of individual single walled carbon nanotube devices using dielectrophoresis, Mater. Express 4 (4) (2014) 263–278.
[29] P. Tiwari, J. Jaiswal, R. Chandra, Hierarchal growth of MoS2@CNT heterostructure for all solid state symmetric supercapacitor: insights into the surface science and storage mechanism, Electrochim. Acta 324 (2019) 134767.
[30] H. Wang, Y. Yang, L. Guo, Nature-inspired electrochemical energy-storage materials and devices, Adva. Energy Mater. 7 (2017) 5.
[31] M.V. Kharlamova, Advances in tailoring the electronic properties of single-walled carbon nanotubes, Prog. Mater. Sci. 77 (2016) 125–211.
[32] K. Zhou, J. Liu, W. Zeng, Y. Hu, Z. Gui, In situ synthesis, morphology, and fundamental properties of polymer/MoS2 nanocomposites, Compos. Sci. Technol. 107 (2015) 120–128.
[33] H. Du, C. Yuan, K. Huang, W. Wang, K. Zhang, B. Geng, A novel gelatin-guided mesoporous bowknot-like Co3O4 anode material for high-performance lithium-ion batteries, J. Mater. Chem. 5 (11) (2017) 5342–5350.
[34] M.R. Islam, S.I. Mollik, Enhanced electrochemical performance of flexible and eco-friendly starch/graphene oxide nanocomposite, Heliyon 6 (10) (2020), e05292.
[35] Z. Wang, et al., Hydrogel electrolytes for flexible aqueous energy storage devices, Adv. Funct. Mater. 28 (48) (2018) 1–30.
[36] S.I. Mollik, R.B. Alam, M.R. Islam, Significantly improved dielectric properties of bio-compatible starch/reduced graphene oxide nanocomposites, Synth. Met. (September) (2020) 116624.
[37] G. Landi, A. Sorrentino, S. Iannace, H.C. Neitzert, Differences between graphene and graphene oxide in gelatin based systems for transient biodegradable energy storage applications, Nanotechnology 28 (2017) 5.
[38] L.J. van der Pauw, A Method of Measuring the Resistivity and Hall Coefficient on Lamellae of Arbitrary Shape, Philips Technical Review, 1958.
[39] Y. Shao, et al., Design and mechanisms of asymmetric supercapacitors, Chem. Rev. 118 (18) (2018) 9233–9280.
[40] L. Liu, et al., Flexible supercapacitor with a record high areal specific capacitance based on a tuned porous fabric, J. Mater. Chem. 4 (33) (2016) 12981–12986.
[41] G. Landi, A. Sorrentino, F. Fedi, H.C. Neitzert, S. Iannace, Cycle stability and dielectric properties of a new biodegradable energy storage material, Nano Energy 17 (2015) 348–355.
[42] R. Sha, S. Badhulika, Few layered MoS2 grown on pencil graphite: a unique single-step approach to fabricate economical, binder-free electrode for supercapacitor applications, Nanotechnology 30 (3) (2019).
[43] M.P. Das, S.P. R, K. Prasad, V. Jv, R. M, Extraction and characterization of gelatin: a functional biopolymer, Int. J. Pharm. Pharmaceut. Sci. 9 (9) (2017) 239.
[44] M.S. Hoque, S. Benjakul, T. Prodpran, Properties of film from cuttlefish (Sepia pharaonis) skin gelatin incorporated with cinnamon, clove and star anise extracts, Food Hydrocolloids 25 (5) (2011) 1085–1097.
[45] A.H.A. Hoseini, M. Arjmand, U. Sundararaj, M. Trifkovic, Significance of interfacial interaction and agglomerates on electrical properties of polymer-carbon nanotube nanocomposites, Mater. Des. 125 (February) (2017) 126–134.
[46] S.H. Park, et al., Modeling the electrical resistivity of polymer composites with segregated structures, Nat. Commun. 10 (1) (2019) 1–11.
[47] Y. Yan, et al., Effect of multi-walled carbon nanotubes on the cross-linking density of the poly(glycerol sebacate) elastomeric nanocomposites, J. Colloid Interface Sci. 521 (2018) 24–32.
[48] M. Pavese, S. Musso, S. Bianco, M. Giorcelli, N. Pugno, An analysis of carbon nanotube structure wettability before and after oxidation treatment, J. Phys. Condens. Matter 20 (2008) 47.
[49] Y. Li, R. Li, X. Fu, Y. Wang, W.H. Zhong, A bio-surfactant for defect control: multifunctional gelatin coated MWCNTs for conductive epoxy nanocomposites, Compos. Sci. Technol. 159 (2018) 216–224.
[50] J.J. Zhang, M.M. Gu, T.T. Zheng, J.J. Zhu, Synthesis of gelatin-stabilized gold nanoparticles and assembly of carboxylic single-walled carbon nanotubes/Au composites for cytosensing and drug uptake, Anal. Chem. 81 (16) (2009) 6641–6648.
[51] C. Sui, et al., Aligned-SWCNT film laminated nanocomposites: role of the film on mechanical and electrical properties, Carbon N. Y. 139 (2018) 680–687.
[52] A.K. Das, A. Mukherjee, K. Baba, R. Hatada, R. Bhowmik, A.K. Meikap, Current-voltage hysteresis behavior of PVA-assisted functionalized single-walled carbon nanotube free-standing film, J. Phys. Chem. C 122 (51) (2018) 29094–29105.
[53] M. Ates, M.A. Serin, S. Calisskan, Electrochemical supercapacitors of PANI/MWCNT, PEDOT/MWCNT and P(ANI-co-EDOT)/MWCNT nanocomposites, Polym. Bull. 76 (6) (2019) 3207–3231.
[54] X.M. Liu, et al., Carbon nanotube (CNT)-based composites as electrode material for rechargeable Li-ion batteries: a review, Compos. Sci. Technol. 72 (2) (2012) 121–144.
[55] A. Sayah, et al., Electrochemical synthesis of polyaniline-exfoliated graphene composite films and their capacitance properties, J. Electroanal. Chem. 818 (April) (2018) 26–34.
[56] S. Wang, et al., Three-dimensional MoS2@CNT/RGO network composites for high-performance flexible supercapacitors, Chem. Eur J. 23 (14) (2017) 3438–3446.
[57] M.A.A. Mohd Abdah, N.A. Zubair, N.H.N. Azman, Y. Sulaiman, Fabrication of PEDOT coated PVA-GO nanofiber for supercapacitor, Mater. Chem. Phys. 192 (2017) 161–169.
[58] X. Ma, et al., A robust asymmetric porous SWCNT/Gelatin thin membrane with salt-resistant for efficient solar vapor generation, Applied Materials Today 18 (2020).
[59] D. Mohapatra, S. Parida, B.K. Singh, D.S. Sutar, Importance of microstructure and interface in designing metal oxide nanocomposites for supercapacitor electrodes, J. Electroanal. Chem. 803 (2017) 30–39.
[60] T.Q. Nguyen, C. Breitkopf, Determination of diffusion coefficients using impedance spectroscopy data, J. Electrochem. Soc. 165 (14) (2018) E826–E831.
[61] X. ying Xu, et al., In-situ temperature regulation of flexible supercapacitors by designing intelligent electrode with microencapsulated phase change materials, Electrochim. Acta 334 (2020).
[62] I. Sifuentes-Nieves, R. Rendón-Villalobos, A. Jiménez-Aparicio, B.H. Camacho-Díaz, G.F. Gutiérrez López, J. Solorza-Feria, Physical, physicochemical, mechanical, and structural characterization of films based on gelatin/glycerol and carbon nanotubes, Int. J. Polym. Sci. 2015 (2015).